Cellulose **12:** 185–196, 2005.
DOI: 10.1007/s10570-004-2785-0

Analysis of the topochemical effects of dielectric-barrier discharge on cellulosic fibers

Lorraine C. Vander Wielen[1], Thomas Elder[2] and Arthur J. Ragauskas[1,*]
*[1]School of Chemistry and Biochemistry, Georgia Institute of Technology, 500 Tenth Street NW, Atlanta, GA 30322-0620, USA; [2]USDA-Forest Service, Southern Research Station, 2500 Shreveport Highway, Pineville, LA 71360, USA; *Author for correspondence (e-mail: arthur.ragauskas@ipst.gatech.edu; phone: +1-404-894-9701; fax: +1-404-894-4778)*

Received 10 May 2004; accepted in revised form 1 September 2004

Key words: AFM, Dielectric-barrier discharge, IGC, Surface roughness, Viscosity, Water retention value.

Abstract

This study investigates the fundamental topochemical effects of dielectric-barrier discharge treatment on bleached chemical pulp and unbleached mechanical pulp fiber surfaces. Fibers were treated with various levels of dielectric-barrier discharge treatment ranging from 0 to 9.27 kW/m^2/min. Changes to the fiber surface topochemistry were investigated by atomic force microscopy (AFM). The AFM studies were complemented by inverse gas chromatography (IGC), contact angle evaluation, poly-electrolyte titration, viscosity testing and determination of water retention value (WRV). The static coefficient of friction and zero-span tensile index of sheets were also evaluated. Low dielectric-barrier discharge treatment levels resulted in increased surface energy and roughness. Fibers treated at high applied power levels showed surface energies and roughness levels near that of reference samples as well as evidence of degradation and decreased fiber swelling.

Abbreviations: AFM – atomic force microscopy; BKP – bleached kraft pulp; IGC – inverse gas chromatography; TMP – thermomechanical pulp; WRV – water retention value.

Introduction

The need to develop new green chemistries that facilitate the development of new materials based on renewable resources has grown into a predominant research challenge over the last two decades (Venselaar 2003). The utilization of lignocellulosics for biofuels, biocomposites (Bruck et al. 2002), and biomaterials (Glasser 1994) is being actively pursued both by academic and industrial researchers. Frequently, an important component in the development of new or improved lignocellulosic materials is the surface chemistry of the fiber. Many schemes for modifying the surface chemistry and morphology of papermaking fibers have been explored. Typically, these methods involve chemical additives (Barzyk et al. 1997; Laine et al. 2000; Henriksson and Gatenholm 2001; Wågberg et al. 2002), enzymes (Viikari et al. 1998), or mechanical treatments (Page 1985; Seth 1999). Dielectric-barrier discharge treatment as a tool for sculpting fiber

topochemistry is of interest given its potential to oxidize the surface of lignocellulosics and its inherent green chemistry. This process requires no chemical additives and has seen increasing industrial interest since it can be performed under atmospheric conditions (Seeböck et al. 2000).

Dielectric-barrier discharge initiated surface treatment occurs when electrons pass from a treatment electrode to a ground electrode with at least one electrode covered by an insulating material, exposing materials in the gap to an atmospheric plasma. This plasma contains a variety of species including electrons with energies great enough to break molecular bonds by collision (Kogelschatz 2003). This results in the creation of excited species including ions, photons, and excited oxygen species including ozone, activated oxygen, free radicals including hydroxide radicals, and free elemental oxygen (Shahin 1966; Cramm and Bibee 1982; Bezigian 1992; Naidis 1997; Egli and Kraus 2003; Kogelschatz 2003). Within the plasma generated by dielectric-barrier discharge, the amount of microfilaments that exist can be increased by increasing either treatment time or watts applied, but individual micro-discharge properties are not altered (Kogelschatz 2003).

Previous dielectric-barrier discharge treatments of synthetic films have been shown to increase polar functional groups at polymer surfaces resulting in increased wettability and surface energy (Roth 2001); while over-oxidation of polyolefin films such as polyethylene, polyethylene terphthalate, and polypropylene results in surface degradation, pinholes, and reduced wettability (Sun et al. 1999). Past studies involving lignocellulosics have shown that dielectric-barrier discharge treatment of cellophane, sized papers, and wood improves wettability and that the roughness of cellophane increases with increased treatment (Brown and Swanson 1971; Sabharwal et al. 1993; Rhen and Viöl 2003). Studies involving oxygen plasma treated pulps indicate increased oxidation and wettability of pulps containing significant amounts of lignin and extractives (Carlsson et al. 1995). In addition, the dielectric-barrier discharge treatment of wood and paper improves the adhesion of paints and glues (Back and Danielsson 1987). As well, the dielectric-barrier discharge of polyethylene improves its adhesion to cellulosic materials (Kim et al. 1970; Kemppi 1996). Dielectric-barrier discharge is also associated with increased surface oxidation of lignocellulosics (Suryani et al. 1980; Sakata et al. 1991; Belgacem et al. 1995; Vander Wielen and Ragauskas 2003) to which improvements in bond strength between pressed plies of cellulose films, bleached sulphite pulp, birch veneer, and paperboard (Goring 1967; Sakata et al. 1991) have been attributed. In addition, the static coefficient of friction of newsprint shows increases with increased dielectric-barrier discharge treatment (Gurnagul et al. 1992). Recently, the ability of dielectric-barrier discharge to accomplish *in situ* grafting of lignocellosics (Vander Wielen and Ragauskas 2004) and provide substantial enhancements in the wet-strength of treated bleached kraft pulp (BKP) and unbleached thermomechanical pulp (TMP) sheets (Vander Wielen et al. 2003) has been demonstrated.

The objective of this study was to perform a comprehensive investigation to characterize the impact of a wide range of applied dielectric-barrier discharge treatment power levels on the surface topochemistry of fully bleached kraft fibers and unbleached mechanical pulp fibers at low and high treatment levels. These two fiber resources were selected as the main constituents of fully bleached kraft fibers are cellulose and hemicellulose; whereas the thermomechanical pulp fibers are composed mainly of cellulose, hemicellulose, and lignin. It was anticipated that the polyphenolic nature of lignin would impact the topochemical reactions initiated by the dielectric-barrier discharge generated plasma.

Materials and methods

Materials

The pulps used in this study are a fully bleached southern pine BKP and a commercial unbleached Norway spruce TMP. The long fiber fraction (6P/35R) of each pulp was collected using a Bauer-McNett fiber fractionator to avoid the detection of differences in surface chemistry which may exist between fines and long fibers. The TMP pulp was Soxhlet extracted with acetone for 24 h. Carbohydrate analysis (Tappi 1996) of the BKP indicated that it consisted of 80.50% glucose, 8.88% xylan, 0.24% galactose, 6.39% mannose, and 0.51% arabinose. The TMP fibers consisted of 48.64% glucose, 4.31% xylan, 1.28% galactose,

9.60% mannose, and 0.57% arabinose. Analysis for lignin content showed that the BKP and TMP contained 0.85 and 26.05% lignin, respectively. All fibers were formed into paper sheets as previously reported (Vander Wielen and Ragauskas 2004). The treated and untreated sheets were acetone extracted in a soxhlet extractor for 24 h prior to atomic force microscopy (AFM) and inverse gas chromatography (IGC) analysis.

Dielectric-barrier discharge treatment

A Sherman Laboratory Treater Station was used to dielectric-barrier discharge treat paper sheets at 0, 0.12, 3.31 and 9.27 kW/m^2/min. The treatment electrode was a ceramic coated aluminum electrode which applied a high voltage across a 1.5 mm gap containing paper samples. The samples were mounted onto an aluminum table which acted as a ground electrode as it passed the sample under the treatment electrode at controlled velocities. The 20 kHz GX-10 power generator was used to convert power to a high frequency alternating current, which was converted to sufficiently high voltages by the HT3 high tension transformer for production of atmospheric plasma.

Atomic force microscopy

In this study, AFM was performed at atmospheric pressure and room temperature in the tapping mode over a 5 μm by 5 μm area with a silicon nitride tip on a Digital Instruments 3100 Scanning Probe Microscope. Samples were held in place by double-sided tape. Resolutions of 512 by 512 pixels were used. For each sample, height images were collected for eight fibers at three locations along the fiber (Mahlberg et al. 1999). The surface roughness was evaluated by the equation

$$R_{\text{rms}} = R(F\Sigma(Z_i - Z_{\text{ave}})^2, N) \qquad (1)$$

where R_{rms} is the root-mean square of the standard deviation for the height (Z) data, Z_{ave} is the average height value, Z_i is the current height value, and N the number of points in the area examined. These values were averaged to give the roughness for each sample. Height images for bleach kraft pulp fibers were also collected.

Poly-electrolyte titration

A published titration method for the determination of surface carboxylic acid groups was applied to quantify the surface charge of the BKP and unbleached TMP fibers (Wägberg et al. 1989). The data plots resulting from titrations were extrapolated to determine the surface acid contents pulp fibers.

Inverse gas chromatography

IGC was performed using teflon columns of length 0.5 m, outside diameter 0.25 in., and inside diameter 0.125 in. that were packed with about 1.0 g of paper sheet material that had been reduced to approximately 1.0 mm square pieces. A Hewlett–Packard 5890 gas chromatograph with a flame ionization detector was used for the chromatography. Helium was the carrier gas, with a flow rate of 15 ml/min. Alkane probe molecules (hexane, heptane, octane, nonane, decane and undecane) were injected at temperatures of 50, 60 and 70 °C. Retention times, based on the average of five injections, were determined relative to methane as an unretained probe. As described in the literature (Shultz and Lavielle 1989), plots of $RT\ln(V_n)$ vs. $a(\gamma^d)^{0.5}$ were constructed, where R = the gas constant, T = temperature (K), a = probe surface area (nm^2), γ^d = dispersive energy of the probe molecule (mJ/m^2), and V_n = relative retention volume in cm^3.

Contact angle

Contact angles of nanopure water on the surface of TMP were determined using the equation for vertical wicking determined by the classic studies of Washburn (1921). The equation

$$h^2/t = r\gamma\cos(\theta)/2\eta \qquad (2)$$

where h is the vertical wicking height, t the time, r the average pore radius, γ the surface tension of water, θ the contact angle, and η the viscosity of water was applied as in past studies modeling the behavior of papermaking fibers and related materials (Winspear 1979; Hodgson and Berg 1988; Danino and Marmur 1994; Hoecker and

Karger-Kocsis 1996; Pillai and Advani 1996; Chen and McMorran 1999; Norris et al. 1999; Shi et al. 2000; Hajnos et al. 2003). Mercury porosimetry was performed by Micromeritics Instrument Corporation to determine the average pore radius. The data collected were used in Equation 2 to estimate the contact angle of nanopure water on TMP fibers.

Water retention value (WRV)

Tappi useful method 256 for WRV determination was applied to BKP and TMP fibers to determine changes in fiber swelling (Tappi 1991). Using this method, fibers were centrifuged at 900 g for 30 min. The fibers were weighed in the wet centrifuged state, oven dried for 24 h, then weighed in the dry state. The WRV was calculated using the equation

$$\mathrm{WRV} = (W_w - W_d)/W_d \qquad (3)$$

where (W_w) is the wet weight and (W_d) the dry weight of the fibers.

Surface roughness

The static coefficient of friction, defined as the ratio of static friction to perpendicular force, was established using a μ Measurements, Inc. Amontons II Model 416 horizontal plane friction testing instrument. The stationary strips were 63.5 mm wide by 152.5 mm long, while the strip mounted on the weighted slide was cut to 63.5 mm × 88.9 mm. The strips were cut from laboratory sheets made from BKP and TMP fibers which were dielectric-barrier discharge treated at 0, 0.12, 3.31 and 9.27 kW/m^2/min. Roughness was also examined by AFM as described above.

Degradation

The viscosities of BKP reference and treated fibers were determined using Tappi Test Method T-230 om-94, as a measure of the relative degree of polymerization of fibers at various treatment levels and zero-span tensile was measured using a Pulmac zero-span tester.

Results and discussion

Atomic force microscopy

AFM has become highly valued for evaluating wood, fiber, and paper surfaces (Hanley and Gray 1994; Böras and Gatenholm 1999; Hanley and Gray 1999; Wistara et al. 1999; Niemi et al. 2002). To explore the fundamental changes in surface properties of the dielectric-barrier discharge treated test sheets, samples were analyzed via AFM. The AFM images showed that qualitatively the untreated kraft fibers (Figure 1a) are similar to those reported in previous studies (Simola et al. 2000; Simola-Gustafsson et al. 2001; Gustafsson et al. 2003), with granular structures visible in the phase images which have been attributed to the deposition of amorphous materials such as hemicellulose. These granular structures are not detected on the surface of the dielectic-barrier discharge treated fibers (Figures 1b–d). The low power dielectric-barrier discharge treatment resulted in significant changes in the fiber surface yielding a rough, fibrillar structure. The fibrils are 20–50 nm in diameter, with most being in the 30–40 nm range. This random fibrillar pattern appears strikingly similar to the primary cell wall layer (Figure 1b) patterns seen in previous AFM studies (Gustafsson et al. 2003). Dielectric-barrier discharge has been applied in remove surface contaminants; a process known as surface cleaning (Goossens et al. 2001). These AFM images indicate that surface cleaning to remove contaminants and amorphous materials from the fiber surface may be occurring, so as to expose the primary cell wall at low dielectric-barrier discharge treatment levels. The medium and high power treatments were also examined by AFM (Figures 1c and d). These differ from the control (Figure 1a) and the low power treatment (Figure 1b) samples. Since the fibrils are parallel in the image of the sample at medium (3.31 kW/m^2/min) treatment, it appears that the primary wall may have been degraded, exposing the middle secondary cell wall (S2) material as the image appears conspicuously similar to S2 layers identified in a previous AFM study of kraft fibers (Hanley and Gray 1999). While fibrils are still discernible in the sample that underwent a medium level of treatment (Figure 1c), they appear more rounded and qualitatively smoother than

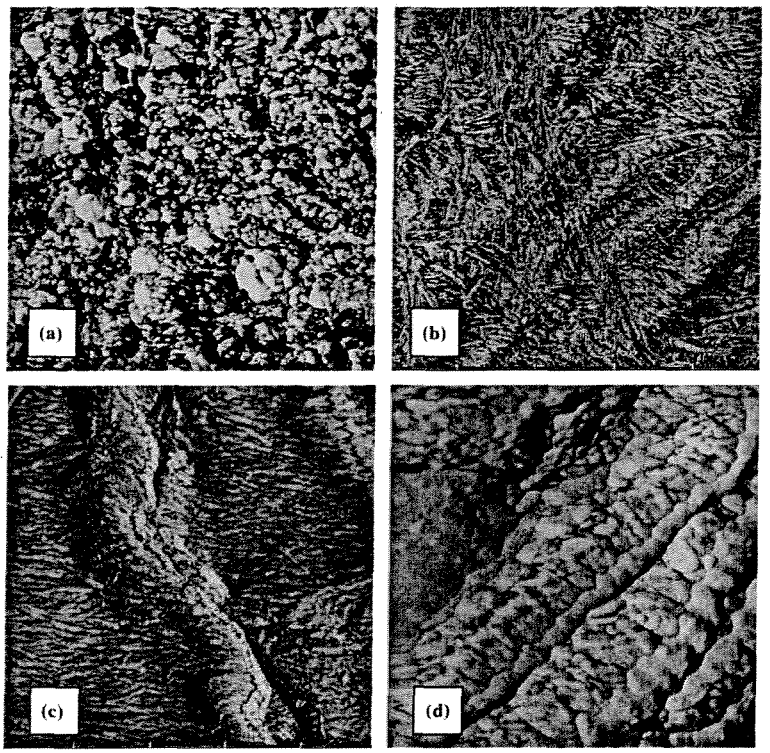

Figure 1. Atomic force microscopy (AFM) phase images of bleached kraft pulp samples at (a) reference condition showing granular surface, (b) at low (0.12 kW/m^2/min) treatment level showing random fibrillar structures, (c) at 3.31 kW/m^2/min or medium treatment showing a smoother parallel fibrillar structure, and (d) at 9.27 kW/m^2/min or high treatment levels showing a smoothed surface.

the sample treated at low applied power levels (Figure 1b). In the sheets treated with the highest power level, the fibrils have completely disappeared, resulting in a much more rounded appearance (Figure 1d).

Phase images from the thermomechanical pulp handsheets are as shown in Figures 2a–d. Visually, these are more internally consistent than the kraft samples. Lignin in the fiber most likely protects unbleached thermomechanical pulp fibers from the extent of dielectric-barrier discharge induced degradation experienced by the bleached kraft fibers. The appearance of the fibril structure on the surface of untreated mechanical pulp fibers detected via AFM is, however, in accord with previous observations (Snell et al. 2001). Although major breakdown of the cell wall layers to reveal underlying layers is not indicated, samples treated at low treatment (0.12 kW/m^2/min) appear as if they may have undergone surface cleaning, as the small amount of granular type materials which appears on the reference sample (Figure 2a) is not observed among the dielectric-barrier discharge treated samples (Figures 2b–2d). In addition, medium (3.31 kW/m^2/min) and high (9.27 kW/m^2/min) applied treatment powers appear to provide smoother fibers.

The plots of root-mean-square roughness determined via AFM show an increase in surface roughness at low treatment levels which declines with increased surface treatment (Figure 3). When compared with the AFM phase images for these fibers, shown in Figures 1 and 2, this data shows an increase in surface roughness which corresponds to the well defined fibrils on the fiber surface seen at low dielectric-barrier discharge treatment levels. The decrease in roughness corresponds with the increasingly smoothed, decreasingly fibrillar appearance of fiber surfaces at higher treatment levels.

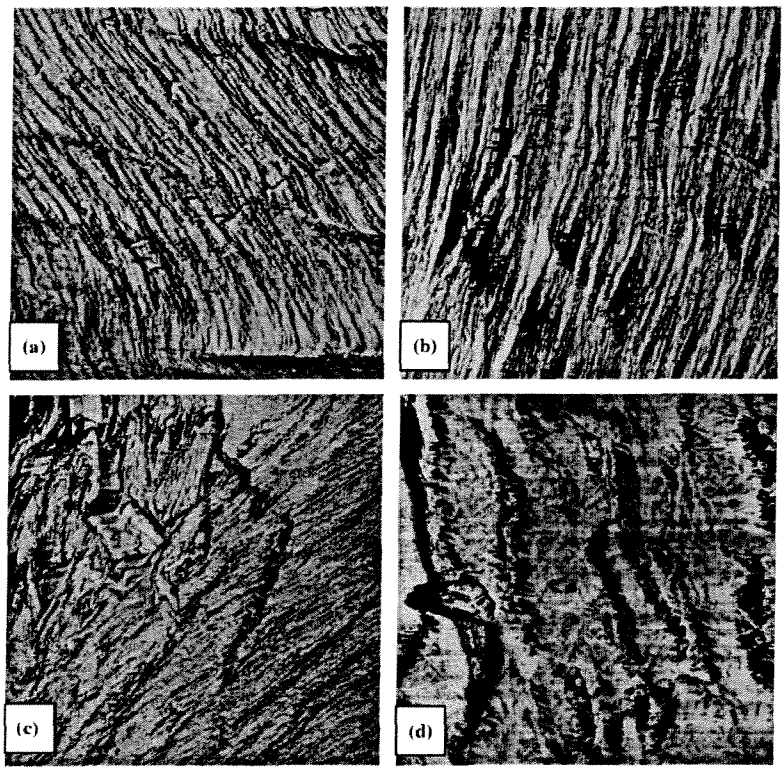

Figure 2. Atomic force microscopy (AFM) phase images of thermomechanical pulp fibers treated at 0 kW/m^2/min (a), 0.12 kW/m^2/min (b), 3.31 kW/m^2/min (c), and 9.27 kW/m^2/min (d) dielectric-barrier discharge treatment levels.

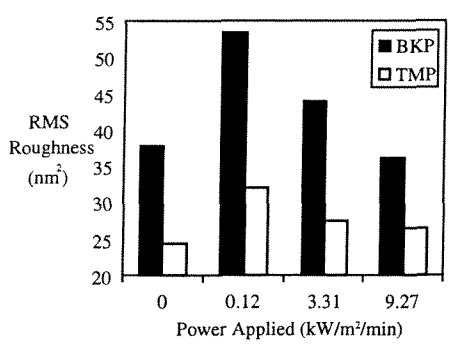

Figure 3. Roughness of bleached kraft (BKP) and thermomechanical pulp (TMP) fibers treated at various treatment dosages evaluated by atomic force microscopy (AFM) in tapping mode.

Poly-electrolyte titration

Poly-electrolyte titrations for the determination of carboxylic acid groups at the surface of kraft and mechanical pulp fibers were performed over a wide array of applied dielectric-barrier discharge treatment power levels, as illustrated in Figure 4. These results confirm an increase in carboxylic acid functionality at low dielectric-barrier discharge treatment power applications, with a return to a level of surface acids similar to that of the reference sample at higher dielectric-barrier discharge power levels. As treatment power increases, the carboxylic acid content returns to the values of the untreated fibers. This change in surface acid groups may be due to an initial oxidative process that at higher treatment energies results in over-oxidation and generation of low molecular weight species that are easily removed by washing with water.

Inverse gas chromatography

IGC was employed to explore changes in surface energy. This method has been applied to

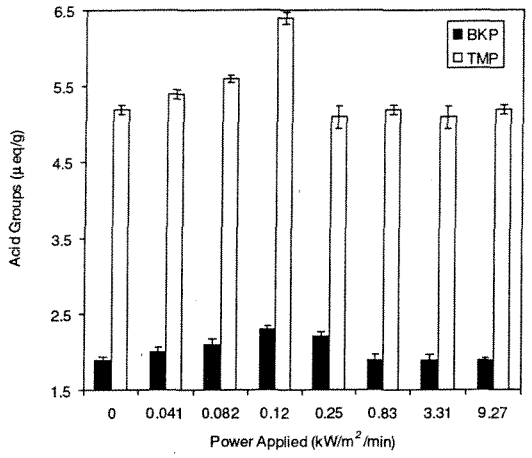

Figure 4. Surface carboxylic acid groups on bleached kraft (BKP) and thermomechanical pulp (TMP) fibers at various dielectric-barrier discharge treatment levels.

examining changes in the surface energy of lignocellulosic fibers in prior studies (Shultz and Lavielle 1989; Felix and Gatenholm 1993; Garnier and Glasser 1994; Jacob and Berg 1994; Liu and Rials 1998; Santos et al. 2001). One study indicates that when hardwood α-cellulose powder is corona-discharge treated, the dispersive surface energy increases with increased treatment (Belgacem et al. 1995). The dispersive surface energies for dielectric-barrier discharge treated kraft and mechanical pulp fibers are summarized in Figure 5. This data has been calculated to 25 °C as in the work of Walinder and Gardner (2000) and Tshabalala et al. (1999). This analysis indicates that the dispersive surface energy of the fibers is maximized at low treatment, suggesting an increase in the polarizability of probe molecules by the fiber surface. This increase in surface energy is maximized at the same treatment energy, 0.12 kW/m^2/min, at which the maximum surface carboxylic acid content was measured; while the decrease and leveling off of the surface energy with increased treatment power applications corresponds to the decrease and leveling off of surface acids seen via polyelectrolyte titration.

Contact angle

Figure 6 provides the contact angles determined using the Washburn equation for the wicking of a

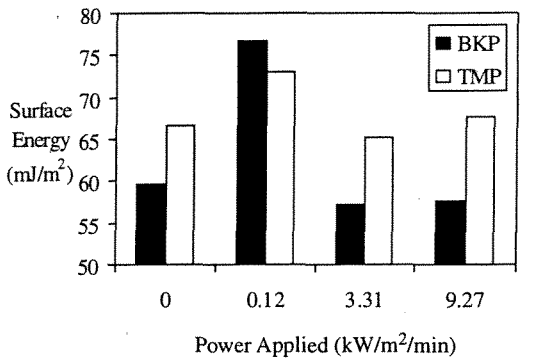

Figure 5. Dispersive surface energies of bleach kraft (BKP) and thermomechanical pulp (TMP) fibers at various dielectric-barrier discharge treatment levels determined via inverse gas chromatography (IGC).

vertical column. The Washburn (1921) equation has been applied to studying the wettability of fibers in numerous studies (Winspear 1979; Hodgson and Berg 1988; Danino and Marmur 1994; Hoecker and Karger-Kocsis 1996; Pillai and Advani 1996; Chen and McMorran 1999; Norris et al. 1999; Shi et al. 2000; Hajnos et al. 2003). In this study, a decreased contact angle at lower treatment levels was observed for the TMP samples. The contact angle began to increase back towards the level of the reference sample with increased dielectric-barrier discharge treatment. This trend is

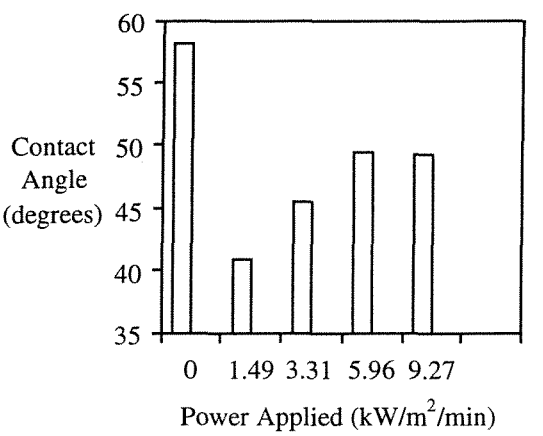

Figure 6. Contact angles of water with the surface of thermomechanical pulp fibers with increased dielectric-barrier discharge treatment, determined using vertical wicking and mercury porosimetry data.

consistent with the trends seen when examining surface acids and surface energy (Figures 4 and 5).

Water retention value

To examine the ability of the fibers to absorb water, WRV for the treated and control sheets were evaluated. WRV analysis (Tappi 1991) for the cold plasma treated BKP indicated an initial increase in WRV at low treatment levels, with a decrease in WRV at higher dielectric-barrier discharge treatment levels (Figure 7). The analysis of thermomechanical pulp fibers showed no change in the WRV with increased dielectric-barrier discharge treatment. The increased WRV of BKP at low treatment levels parallels the spike in acid groups and surface energy seen at low treatment levels (Figures 4 and 5).

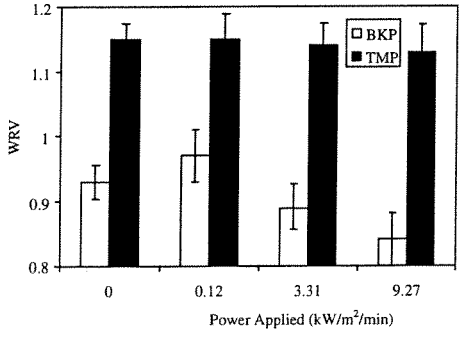

Figure 7. Water retention value (WRV) of bleached kraft (BKP) and thermomechanical pulp (TMP) fibers as the applied dielectric-barrier discharge power was increased.

Coefficient of friction

Examinations of surface roughness properties yielded similar trends as observed for surface energy, increasing at lower dielectric-barrier discharge treatment levels and smoothing at higher treatment. As seen in Figure 3, the plots of root-mean-square roughness determined employing AFM show trends that are strikingly similar to those from the analysis of surface acids (Figure 4) and the dispersive component of surface energy (Figure 5). The root-mean-square average surface roughness of the fibers is at its largest value with dielectric-barrier discharge treatment at 0.12 kW/m^2/min, as were surface acids and surface energy, with similar decreases dielectric-barrier discharge treatment was increased. The coefficient of friction for the kraft and thermomechanical pulp sheets followed trends similar, but not identical, to the roughness trends of those demonstrated using atomic force microscopy in tapping mode. Figure 8 shows that the low dielectric-barrier discharge treatment level results in a great increase in the static coefficient of friction of both BKP and

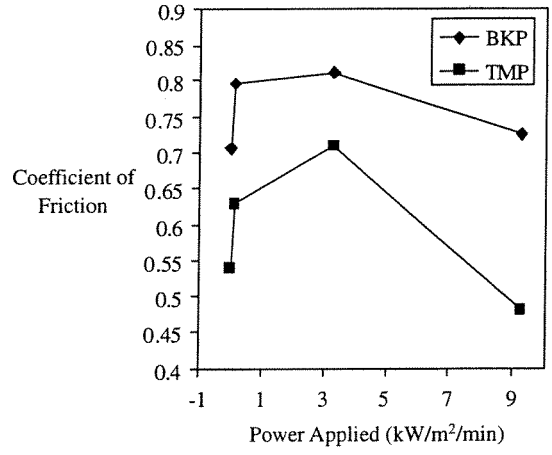

Figure 8. The static coefficient of friction (COF) of bleached kraft pulp (BKP) and thermomechanical pulp (TMP) samples at various dielectric-barrier discharge treatment levels.

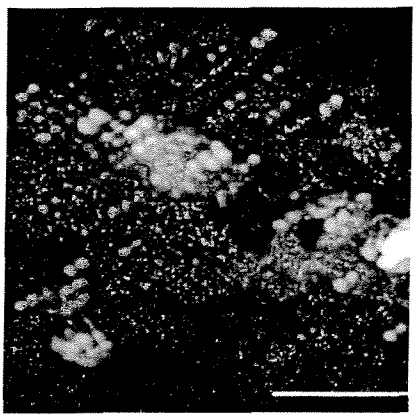

Figure 9. Atomic force microscopy (AFM) height image of 5.0 μm × 5.0 μm bleached kraft pulp sample dielectric-barrier discharge treated at high (9.27 kW/m^2/min) intensity, white bar = 1.0 μm.

TMP fibers. However, at the greatest applied power level, 9.27 kW/m^2/min, the coefficient of friction of the treated and reference bleached kraft sheets were similar to the untreated sheets. In the case of the thermomechanical pulp sheets, high treatment levels provided a coefficient of friction even lower than that of the reference sample.

The AFM height image (Figure 9) taken from the surface of highly treated BKP fibers indicated the presence of bumps or nodules on the surface of fibers treated at a high applied treatment level (9.27 kW/m^2/min) despite the overall coefficient of friction and AFM roughness, which indicate that higher treatment levels provide fibers that are much smoother than those treated at low dielectric-barrier discharge treatment levels. These surface nodules are appreciably similar to those seen when an RF oxygen plasma was applied to Whatman filter paper (Mahlberg et al. 1999). It is possible that these nodules form due to surface etching, localized melting, or the degradation and redistribution of the surface components of kraft fibers.

Degradation

It was of interest to determine if the surface analysis studies correlated to common properties that suggest degradation such as pulp viscosity and zero-span tensile. As summarized in Figure 10, we observed a decrease in the viscosity of BKP fibers and decreases in the zero-span tensile of BKP and TMP sheets with increased dielectric-barrier discharge treatment dosages. The decreases in viscosity (Figure 10), along with inspection of AFM images for bleached kraft fibers (Figures 1a–d), indicate an increased surface degradation effect with increased dielectric-barrier discharge treatment. Specifically, the AFM visualization suggests that surface cleaning and removal/degradation of polysaccharides at the fiber surface may occur. The decreased zero-span tensile adds further evidence for the degradation of fibrous material.

Conclusions

Results of surface analysis indicate that at low dielectric-barrier discharge treatment the surface

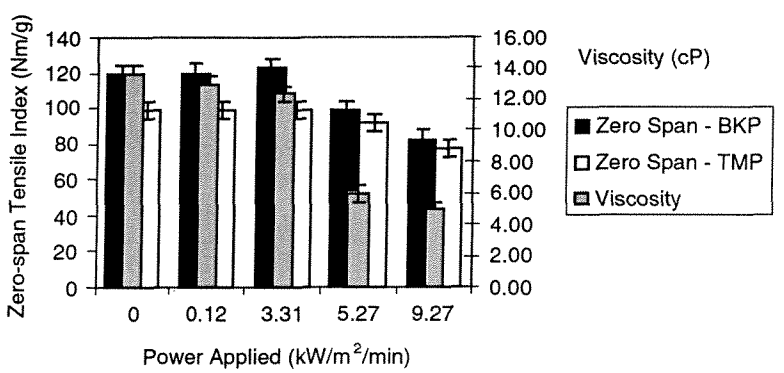

Figure 10. Viscosity of bleached kraft (BKP) and zero-span tensile strength of BKP and thermomechanical pulp (TMP) sheets decrease with increased dielectric-barrier discharge treatment.

energy, carboxylic acid content, surface roughness and the coefficient of friction of BKP and unbleached TMP fibers are increased. At higher treatment levels, these effects disappear as fiber surfaces appear to become smoother along with the formation of nodules on the bleached kraft pulp fibers. In addition, the coefficient of friction and RMS surface roughness decrease, and the fiber surface chemistry becomes similar to that of the untreated fiber in terms of fiber charge and surface energy. However, in terms of fiber degradation, greater degradation occurs as dielectric-barrier discharge treatments are increased. The increased hydrophilicity of BKP at low treatment levels is likely due to increased oxidation as evidenced by increases in surface acids and fiber surface cleaning as suggested by AFM images; while increased surface smoothness and decreased WRV and surface energy are seen at high treatment levels. The overall results of this study indicate a fine balance between oxidative reactions to increase wettability, oxidative degradation and decreased wettability.

Acknowledgements

The authors wish to acknowledge the support of the member companies of the Institute of Paper Science and Technology at the Georgia Institute of Technology. Portions of this work are being used by L. Vander Wielen as partial fulfillment of the requirements for graduation from the Institute of Paper Science and Technology at the Georgia Institute of Technology, Atlanta, Georgia.

References

Back E.L. and Danielsson S. 1987. Oxidative activation of wood and paper surfaces for bonding and for paint adhesion. Nord. Pulp Pap. Res. J. 53–62.

Barzyk D., Page D.H. and Ragauskas A.J. 1997. Acidic-group topochemistry and fiber-to-fiber specific bond strength. J. Pulp Pap. Sci. 23: J59–J61.

Belgacem M.N., Czeremuszkin G. and Sapieha S. 1995. Surface characterization of cellulose fibers by XPS and inverse gas chromatography. Cellulose 2: 145–157.

Bezigian T. 1992. The effect of corona discharge onto polymer films. Tappi J. 75: 139–141.

Böras L. and Gatenholm P. 1999. Surface composition and morphology of CTMP fibers. Holzforschung 53: 188–194.

Brown P.F. and Swanson J.W. 1971. Wetting properties of cellulose treated in a corona discharge. Tappi J. 54: 201–208.

Bruck H.A., Evans J.J. and Peterson M.L. 2002. The role of mechanics in biological and biologically inspired materials. Exp. Mech. 42: 361–371.

Carlsson C., Ström G. and Annergren G. 1995. Water sorption and surface composition of untreated or oxygen plasma-treated chemical pulps. Nord. Pulp Pap. Res. J. 10: 17–23.

Chen D. and McMorran D. 1999. Use of the DCA technique to measure the wettability of porous materials. Am. Lab. 31: 35–37.

Cramm R.H. and Bibee D.V. 1982. Theory and practice of corona treatment for improving adhesion. Tappi J. 65: 75–78.

Danino D. and Marmur A. 1994. Radial capillary penetration in to paper: Limited and unlimited liquid reservoirs. J. Colloid Interf. Sci. 166: 245–250.

Egli W. and Kraus M. 2003. Shortest paths in chemical kinetic applications. Phys. Chem. Chem. Phys. 5: 3916–3920.

Felix J.M. and Gatenholm P. 1993. Characterization of cellulose fibers using inverse gas chromatography. Nord. Pulp Pap. Res. J. 8: 200–203.

Garnier G. and Glasser W.G. 1994. Measurement of the surface free energy of amorphous cellulose by alkane adsorption: a critical evaluation of inverse gas chromatography. Langmuir 46: 168–180.

Glasser W.G. 1994. Chemical products from lignocellulosics. MRS Bull. 19: 46–48.

Goossens O., Dekempeneer E., Vangeneugden D. and de Leest R. 2001. Application of atmospheric pressure dielectric barrier discharges in deposition, cleaning and activation. Surf. Coat. Tech. 142–144: 474–481.

Goring D.A.I. 1967. Surface modification of cellulose in a corona discharge. Pulp Pap. Mag. Can. 68: T372–T376.

Gurnagul N., Ouchi M.D., Dunlop-Jones N., Sparkes D.G. and Wearing J.T. 1992. Factors affecting the coefficient of friction of paper. J. Appl. Poly. Sci. 46: 805–814.

Gustafsson J., Ciovica L. and Peltonen J. 2003. The ultrastructure of spruce kraft pulps studies by atomic force microscopy (AFM) and X-ray Photoelectron Spectroscopy (XPS). Polymer 44: 661–670.

Hajnos M., Jozefaciuk G., Sokolowska Z., Greiffenhagen A. and Wessolek G. 2003. Water storage, surface and the structural properties of sandy forest humus horizons. J Plant Nutr. Soil Sci. 166: 625–634.

Hanley S.J. and Gray D.G. 1994. Atomic force microscopy images of black spruce wood sections and pulp fibers. Holzforschung 48: 29–34.

Hanley S.J. and Gray D.G. 1999. AFM images in air and water of kraft pulp fibers. J. Pulp Pap. Sci. 25: 196–200.

Henriksson Å and Gatenholm P. 2001. Controlled assembly of glucoronoxylans onto cellulose fibers. Holzforschung 55: 494–502.

Hodgson K.T. and Berg J.T. 1988. Wettability of single wood fibers and their relationship to absorbency. Wood Fiber Sci. 20: 3–17.

Hoecker F. and Karger-Kocsis J. 1996. Surface energetics of carbon fibers and its effect on the mechanical performance of CF/EP composites. J. Appl. Polym. Sci. 59: 139–153.

Jacob P.N. and Berg J.C. 1994. Acid-base surface energy characterization of microcrystalline cellulose and two wood pulp fiber types using inverse gas chromatography. Langmuir 10: 3086–3093.

Kemppi A. 1996. Studies on adhesion between paper and low-density polyethylene's influence on the natural components in paper. Pap. Puu 78: 610–617.

Kim C.Y., Suranyi G. and Goring D.A.I. 1970. Corona induced bonding of synthetic polymers to cellulose. J. Polym. Sci. 30: 533–542.

Kogelschatz U. 2003. Filamentary and diffuse barrier discharges: their history, discharge physics and industrial applications. Plasma Chem. Plasma Proc. 23: 1–46.

Laine J., Lindström T., Nordmark G.G. and Risinger G. 2000. Studies on the topochemical modification of cellulosic fibers, Part 1. Chemical conditions for the attachment of carboxylmethyl cellulose onto fibers. Nord. Pulp Pap. Res. J. 15: 520–526.

Lui F.P. and Rials T.G. 1998. Relationship of wood surface energy to surface composition. Langmuir 14: 536–541.

Mahlberg R., Niemi J.E.-M., Denes F.S. and Rowell R.M. 1999. Application of AFM to the adhesion studies of oxygen-plasma-treated polypropylene and lignocellulosics. Langmuir 15: 2985–2992.

Naidis G.V. 1997. Modeling of plasma chemical processes in pulsed corona discharges. J. Phys. D: Appl. Phys. 30: 1214–1218.

Niemi H., Paulapuro H. and Mahlberg R. 2002. Review: application of scanning probe microscopy to wood, fiber and paper research. Pap. Puu 84: 389–406.

Norris D.A., Puri N., Labib M.E. and Sinko P.J. 1999. Determining the absolute surface hydrophobicity of microparticles using thin layer wicking. J Control. Release 59: 173–185.

Page D.H. 1985. The mechanism of strength development of dried pulps by beating. Svensk Papperstid. 3: R30–R35.

Pillai K.M. and Advani S.G. 1996. Wicking across a fiber bank. J. Colloid Interf. Sci. 183: 100–110.

Rhen P. and Viöl W. 2003. Dielectric barrier discharge treatments at atmospheric pressure for wood surface modification. Holz als Roh- und Werkstoff 61: 145–150.

Roth J.R. 2001. Industrial Plasma Engineering. Applications to Nonthermal Plasma Processing Vol. 2. Institute of Physics Publishing, Bristol, UK, pp. 122–125.

Sabharwal H.S., Denes F., Nielssen L. and Young R.A. 1993. Free-radical formation in jute from argon plasma treatment. J. Agric. Food Chem. 41: 2202–2207.

Sakata I., Morita M., Furuichi H. and Kawaguchi Y. 1991. Improvement of ply bond strength of paperboard by corona treatment. J. Appl. Polym. Sci. 42: 2099–2104.

Santos J.M.R.C.A., Gil M.H., Portugal A. and Guthrie J.T. 2001. Characterization of the surface of a cellulosic multipurpose office paper by inverse gas chromatography. Cellulose 8: 217–224.

Seeböck R., Esrom H., Charbonnier M. and Romand M. 2000. Modification of polyimide in barrier discharge air plasmas: chemical and morphological effects. Plasmas Polym. 5: 103–118.

Seth R.S. 1999. Beating and refining response of some reinforcement pulps. Tappi J. 82: 147–151.

Shahin M.M. 1966. Mass-spectrometric studies of corona discharges in air at atmospheric pressures. J. Chem. Phys. 45: 2600–2605.

Shi S.Q., Tze W.T. and Gardner D.J. 2000. A new model to determine contact angles on swelling polymer particles by the column wicking method. J. Adhesion Sci. Technol. 14: 301–314.

Shultz J. and Lavielle L. 1989. Inverse Gas Chromatography. In: Lloyd D.R., Ward T.C., Schrieber H.P. and Pizaña C.C. (eds), ACS Symposium Series 391. American Chemical Society, Washington, DC, pp. 185–202.

Simola-Gustafsson J., Hortling B. and Peltonen J. 2001. Scanning probe microscopy and enhanced data analysis on lignin and elemental-chlorine free or oxygen-delignified pine kraft pulp. Colloid Polym. Sci. 279: 221–231.

Simola J., Malkavaara P. and Peltonen J. 2000. Scanning probe microscopy of pine and birch kraft pulp fibers. Polymer 41: 2121–2126.

Snell R., Groom L.H. and Rials T.G. 2001. Characterizing the surface roughness of thermomechanical pulp fibers with atomic force microscopy. Holzforschung 55: 511–520.

Sun C.Q., Zhang D. and Wadsworth L.C. 1999. Corona treatment of polyolefin films – A review. Adv. Polym. Tech. 18: 171–180.

Suranyi G., Gray D.G. and Goring D.A.I. 1980. The effect of corona discharge on wettability of aged corrugating medium. Tappi J. 63: 153–154.

TAPPI Test Methods. 1996. Tappi Press, Atlanta, GA.

TAPPI Useful Methods 1991. Tappi Press, Atlanta, GA, p. 54–56.

Tshabalala M., Denes A. and Williams S. 1999. Correlation of water vapor adsorption behavior of wood with surface thermodynamic properties. J. Appl. Polym. Sci. 73: 399–407.

Vander Wielen L.C. and Ragauskas A.J. 2003. Dielectric discharge: a concatenated approach to fiber modification. Proceedings of the 12th International Symposium on Wood and Pulping Chemistry, Vol. 1, Madison, WI, pp. 272–276.

Vander Wielen L.C., Page D.H. and Ragauskas A.J. 2003. Impact of dielectric-barrier discharge on bonding. International Paper Physics Conference Pre-prints, PAPTAC, Victoria, pp. 347–349.

Vander Wielen L.C. and Ragauskas A.J. 2004. Grafting of acrylamide onto cellulosic fibers via dielectric-barrier discharge. Eur. Polym. J. 40: 477–482.

Venselaar J. 2003. Sustainable growth and chemical engineering. Chem. Eng. Technol. 26: 868–874.

Viikari L., Harkki T., Niku-Paavlova M.-L., Buchert J. and Popplus-Levlin K. 1998. Oxidative enzymes for fiber modification. Proceedings of the 7th International Conference on Biotechnology in the Pulp and Paper Industry, Vancouver, Canada, pp. A121–A124.

Wägberg L., Forsberg S., Johansson A. and Juntti P. 2002. Engineering of fiber surface properties by application of the polyelectrolyte multilayer concept. Part 1. Modification of paper strength. J. Pulp Pap. Sci. 8: 222–228.

Wägberg L., Odberg, L. and Glad-Nordmark G. 1989. Charge determination of porous substrates by polyelectrolyte absorption. Nord. Pulp Pap. Res. J. 2: 71–76.

Walinder M. and Gardner D. 2000. Surface energy of extracted and non-extracted Norway spruce wood particles studied by inverse gas chromatography (IGC). Wood Fiber Sci. 32: 478–488.

Washburn E.W. 1921. Dynamics of capillary flow. Phys. Rev. 17: 374–375.

Winspear S. 1979. The characterization of liquid acceptance by paper. Appita 33: 25–32.

Wistara N., Zhang X. and Young R.A. 1999. Properties and treatments of pulps from recycled paper. Part II. Surface properties and crystallinity of fibers and fines. Cellulose 6: 325–428.